GEOLOGY | THE GEOLOGICAL SOCIETY OF AMERICA®

https://doi.org/10.1130/G49318.1

Manuscript received 24 May 2021
Revised manuscript received 18 July 2021
Manuscript accepted 23 July 2021

Published online 20 September 2021

Rivers in reverse: Upstream-migrating dechannelization and flooding cause avulsions on fluvial fans

Douglas A. Edmonds[1], Harrison K. Martin[1], Jeffery M. Valenza[1], Riley Henson[1], Gary S. Weissmann[2], Keely Miltenberger[2], Wade Mans[2], Jason R. Moore[3], Rudy L. Slingerland[4], Martin R. Gibling[5], Alexander B. Bryk[6] and Elizabeth A. Hajek[4]

[1]Indiana University, Department of Earth and Atmospheric Sciences, 1001 E. 10th Street, Bloomington, Indiana 47405-1405, USA
[2]University of New Mexico, Department of Earth and Planetary Sciences, MSC 03 2040, 1 University of New Mexico, Albuquerque, New Mexico 87131-0001, USA
[3]University of New Mexico, Honors College, MSC 06 3890, 1 University of New Mexico, Albuquerque, New Mexico 87131-0001, USA
[4]Pennsylvania State University, Department of Geosciences, Deike Building, University Park, Pennsylvania 16802, USA
[5]Dalhousie University, Department of Earth and Environmental Sciences, 1459 Oxford Street, P.O. Box 15000, Halifax, Nova Scotia B3H 4R2, Canada
[6]Department of Earth and Planetary Science, 307 McCone Hall, University of California, Berkeley, California 94720-4767, USA

ABSTRACT

The process of river avulsion builds floodplains and fills alluvial basins. We report on a new style of river avulsion identified in the Landsat satellite record. We found 69 examples of retrogradational avulsions on rivers of densely forested fluvial fans in the Andean and New Guinean alluvial basins. Retrogradational avulsions are initiated by a channel blockage, e.g., a logjam, that fills the channel with sediment and forces water overbank (dechannelization), which creates a chevron-shaped flooding pattern. Dechannelization waves travel upstream at a median rate of 387 m/yr and last on average for 13 yr; many rivers show multiple dechannelizing events on the same reach. Dechannelization ends and the avulsion is complete when the river finds a new flow path. We simulate upstream-migrating dechannelization with a one-dimensional morphodynamic model for open channel flow. Observations are consistent with model results and show that channel blockages can cause dechannelization on steep (10^{-2} to 10^{-3}), low-discharge (~10^{1} m^3 s^{-1}) rivers. This illustrates a new style of floodplain sedimentation that is unaccounted for in ecologic and stratigraphic models.

INTRODUCTION

The repeated avulsion of rivers to new locations influences the formation and topographic evolution of floodplains. River avulsion style impacts floodplain filling because, during relocation, some avulsions deposit sediment and prograde across their floodplains (Smith et al., 1989; Mohrig et al., 2000; Stouthamer and Berendsen, 2000), whereas others reoccupy a preexisting channel or incise new channels (Mohrig et al., 2000; Hajek and Edmonds, 2014). These different styles impact forest biodiversity on floodplains (Collins et al., 2012; Wohl, 2020) and the stratigraphic architecture of fluvial deposits (Kraus, 1996; Jones and Hajek, 2007). Despite these important impacts, our understanding of avulsion style is limited to a few well-documented cases because avulsions occur infrequently. However, recent work has shown that avulsions are common enough on fluvial fans in sedimentary basins to be captured in the Landsat satellite record (Buehler et al., 2011; Weissmann et al., 2015; Edmonds et al., 2016; Lombardo, 2016; Valenza et al., 2020).

On fluvial fans in the Andean and New Guinean sedimentary basins, we recognize a new style of river avulsion initiated by an upstream-migrating wave of overbank flooding (dechannelization). Unlike successive, upstream-migrating avulsion nodes (Mackey and Bridge, 1995) or upstream-propagating effects that change fluxes in a channel network (Kleinhans et al., 2012), the upstream migration observed here occurs on a single channel during a single avulsion and is the mechanism that forces flow from the channel onto the floodplain. We present a data set of 69 "retrogradational" avulsions observed in Landsat data (1984–2020 CE), so-called because the overbank flooding and sedimentation moves upstream. We describe a conceptual model for this process based on high-resolution serial imagery and test it with a numerical model that solves the one-dimensional (1-D) St. Venant equations and sediment mass conservation along a river centerline. Our modeling is consistent with field data and shows that channel blockages can induce upstream-migrating dechannelization on steep (10^{-2} to 10^{-3}), low-discharge (~10^{1} m^3 s^{-1}) rivers.

A CONCEPTUAL MODEL FOR RETROGRADATIONAL AVULSIONS

The process of retrogradational avulsion involves two phases: upstream-migrating dechannelization, and flow-path selection. Exactly what initiates the first phase is unknown because it is not captured in available imagery. But once the overbank flow and dechannelization start, all avulsions follow a progression like avulsion R3.2 from Papua New Guinea (Fig. 1; see Table S1 in the Supplemental Material[1]). In 2003, the already sediment-filled channel forced flow overbank and created a chevron-shaped zone of dead vegetation and

[1]Supplemental Material. Dataset describing the retrogradational avulsions in this study, including beginning and ending locations and dates, and geomorphic, hydrological, and topographic measurements. Please visit https://doi.org/10.1130/GEOL.S.15832101 to access the supplemental material, and contact editing@geosociety.org with any questions.

CITATION: Edmonds, D.A., et al., 2021, Rivers in reverse: Upstream-migrating dechannelization and flooding cause avulsions on fluvial fans: Geology, v. 50, p. 37–41, https://doi.org/10.1130/G49318.1

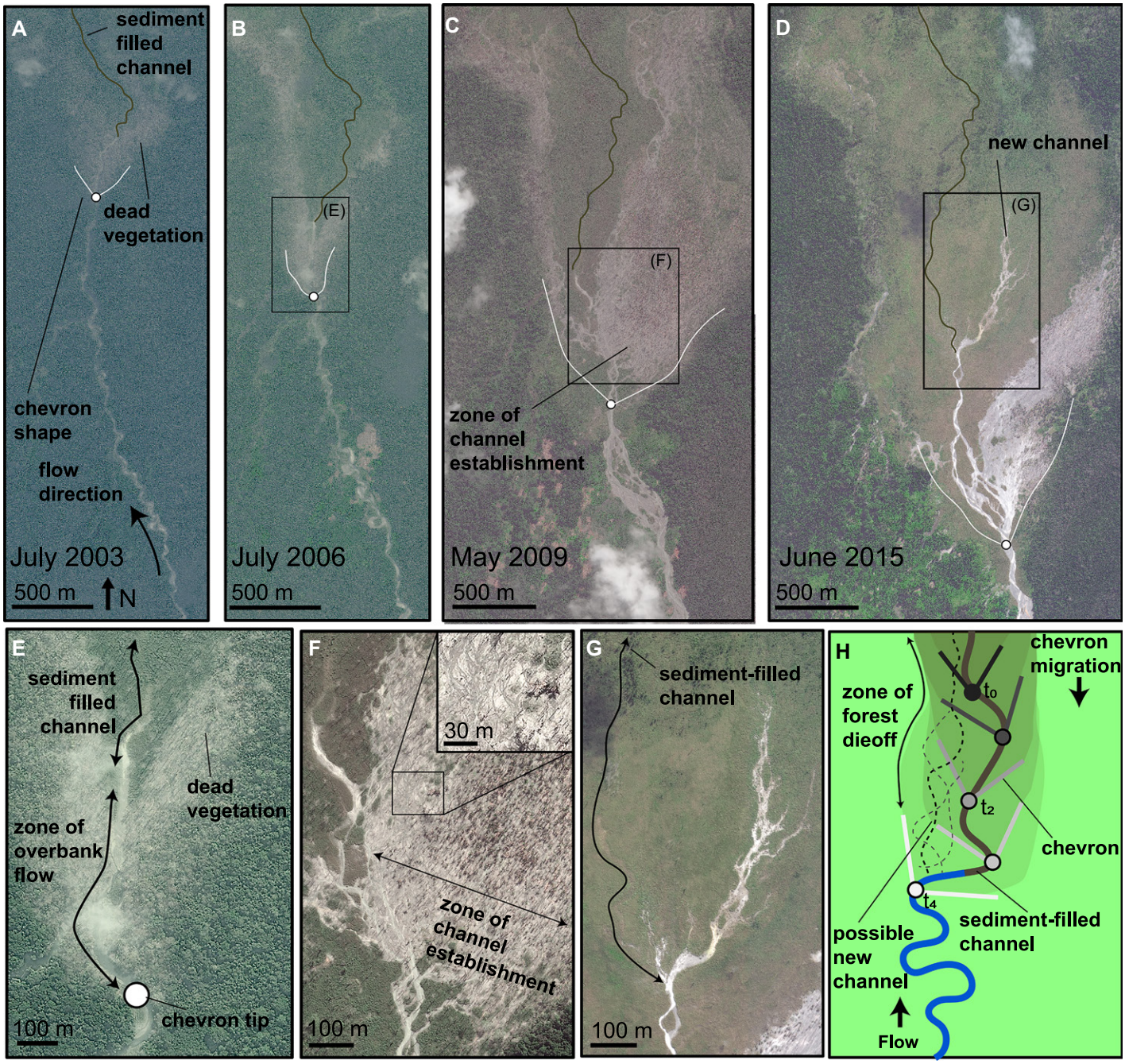

Figure 1. Temporal evolution of retrogradational avulsion R3.2 in Papua New Guinea (see text for details). Tip of the chevron in (A) is at 9.435°S, 149.095°E. Curved traces (inset in F) are scours around the trees. (H) Schematic representation. Satellite images in A, B, and E are from QuickBird2 satellite; images in C and F are from GeoEye-1 satellite, and images in D and G are from WorldView3. Imagery Copyright 2021 Maxar, Inc.

trees, and the chevron opened downstream (Fig. 1A). This chevron was observed on every avulsion and is a diagnostic feature of retrogradational avulsions. Dead vegetation indicates that the chevron tip, and hence the zone of overbank flow, started upstream of the sediment-filled channel (Figs. 1B and 1E). From 2003 to 2006, continued sedimentation in the channel caused the chevron-shaped zone of overbank flow to migrate upstream 640 m (Figs. 1A and 1B), leaving the downstream parent channel filled with sediment.

During the second phase, the channel selects a new flow path and completes the retrogradational avulsion. Once dechannelization begins, avulsion is inevitable because the original channel downstream of the chevron is sediment-filled. The overbank flow may annex a preexisting channel or construct one through progradation. The new flow path commonly forms downstream of the chevron by channelization around trees, which occurred in 2009 when the chevron of R3.2 enlarged, probably due to a levee crevasse (Figs. 1C and 1F inset). A channel pathway amongst the trees enlarged, and by 2015 a new channel had formed (Figs. 1D and 1G). The terminus of the new channel has a splay-like zone that propagates downstream, and it will eventually link up with an existing channel, not necessarily the original parent channel, to complete the avulsion.

STATISTICS OF RETROGRADATIONAL AVULSIONS

Retrogradational avulsions in the Andean and New Guinean basins mostly occur on narrow,

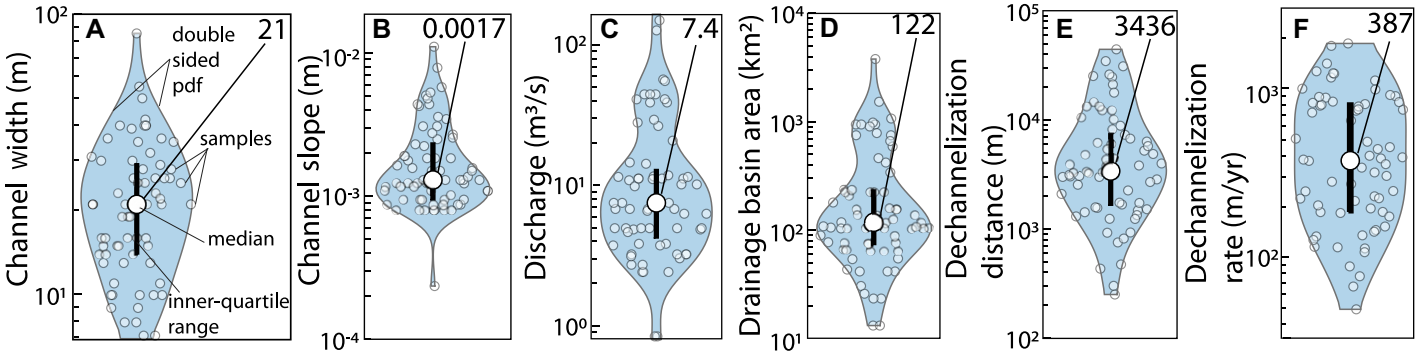

Figure 2. Statistics for retrogradational avulsions. (A) Channel width from high-resolution imagery upstream of the avulsion. (B) Channel slope from a linear regression of elevation from the beginning to ending location using either Shuttle Radar Topography Mission data or Google Earth™. (C,D) Discharge and drainage basin area from RiverATLAS (Linke et al., 2019) measured at the starting location of each avulsion. (E,F) Dechannelization distance measured along the river centerline from the beginning to ending location; dechannelization rate is that distance divided by duration. Blue areas are double-sided probability distribution functions (pdf). See the Supplemental Material and Table S1 for more detail (see footnote 1).

steep rivers with small discharges (Figs. 2A–2D) These rivers are mostly on small fans or interfans between megafans. The channels are relatively narrow (7–85 m range, average 23 m), but three occur on larger fluvial fans (R46; chevron begins at 14.4708°S, 66.3524°W) or as part of crevasse splays (R34.1 [16.2666°S, 65.8723°W] and R34.2 [16.2996°S, 65.875°W]). Many of the rivers experience multiple retrogradational avulsions. The 69 examples occur on 44 unique rivers, 41% of which experienced multiple avulsions that initiated on the same river reach. Three rivers experienced four different retrogradational avulsions from 1984 to 2020. Measurements, locations, and data are included in the Supplemental Material.

Averaged across all events, the waves of dechannelization lasted for 13 yr and travelled at 387 m/yr (Figs. 2E and 2F; Table S1), and faster avulsions dechannelized longer distances. In one exceptional event (R28), the dechannelization wave moved upstream for ~35 km, and through a tributary junction at 1500 m/yr, and in another event, multiple channels on a fan (samples R3–R7) seemed to dechannelize simultaneously (see Supplemental Movies S1 and S2). Estimates of the dechannelization length and duration are minimum values since some avulsions were ongoing at the start or end of the Landsat data period.

INITIATION OF DECHANNELIZATION

In the remote sensing data, we do not observe what initiates dechannelization, but two explanations are explored here. Upstream-migrating dechannelization has been documented on the Okavango fan (McCarthy et al., 1992), terminal splay fans in Bolivia (Donselaar et al., 2013), floodout zones in Australia (Tooth, 2000), and in lab experiments (e.g., Hamilton et al., 2013). In these examples, reduced stream capacity from flow expansion, evaporation, or water infiltration into the subsurface caused the channel to fill with sediment and initiated dechannelization. For instance, in lab experiments dechannelization occurs through flow expansion at the fan margin or at an abrupt transition from steep to gentle slopes (Reitz and Jerolmack, 2012; Van Dijk et al., 2012; Hamilton et al., 2013). While more conclusive tests are needed, it seems that the observed retrogradations are not associated with slope breaks or reduced capacity; for example, avulsions R3.1 and R3.2 occur in steep and gentle portions of the same river (Fig. S1).

Alternatively, dechannelization could be initiated by a channel blockage that forces water overbank. Observations of avulsion R19.3 (Fig. S2) and at other rivers in Bolivia (Lombardo, 2017) show that woody debris helps propagate dechannelization. In steep and narrow rivers, woody debris will not travel far and may create channel-spanning jams (Abbe and Montgomery, 2003; Wohl, 2011; Ruiz-Villanueva et al., 2016) that could cause dechannelization. Once logjams form, they create a local backwater (Geertsema et al., 2020) and enough bed aggradation to cause an avulsion (Wohl, 2011, 2020; Phillips, 2012). Because wood is abundant on these forested fans, we developed a conceptual numerical model to test whether a channel blockage can initiate dechannelization (Fig. 1H).

NUMERICAL MODELING OF DECHANNELIZATION

Our model explores a river reach using the 1-D St. Venant equations with overbank flow loss and conservation of bed sediment (details are provided in the Supplemental Material). Our experiments started at a river reach with steady, uniform flow. Then we placed a Gaussian-shaped sediment blockage in the middle of the channel (Fig. 3). In the field examples, the blockage would be made of logs, but the mobility of jammed wood is unknown, and logjams are hydrodynamically similar to sediment blockages (Geertsema et al., 2020). Overbank flow caused by the blockage was computed with a side weir formulation (Ranga Raju et al., 1979; Hager, 1987), and when the channel depth was less than 5 cm, we forced it to be dry (Medeiros and Hagen, 2013). We computed 648 runs to explore the conditions that lead to dechannelization across the slopes, widths, and discharges observed for retrogradational avulsions (Figs. 2A–2C). For each unique combination, we simulated five different nondimensional blockage heights (b^*) from 0.5 to 1, where $b^* = \frac{b_h}{h_o}$. b_h is the height of the blockage and h_o is the normal flow depth without a blockage present.

Our model reproduces upstream-migrating dechannelization through a positive feedback (Fig. 3A). The blockage decelerates flow and creates a local backwater that raises the water surface upstream, which leads to overbank flow (Fig. 3B). In the field example, this backwater effect may be why the chevron tip is upstream of the sediment-filled channel (Figs. 1B and 1E). The overbank flow reduces discharge and sediment transport capacity in the channel, causing deposition and upstream accretion of the blockage, forcing the overbank flow to migrate upstream (Fig. 3B). This dechannelization continues indefinitely in the model but stops in the field examples when overbank flow finds a new flow path. The model predicts that dechannelization can happen on rivers with small discharges and steep slopes (Fig. 4) because these conditions maximize backwater height relative to the flow depth, and therefore maximize the proportion of incoming discharge lost overbank.

Not all conditions lead to dechannelization (Figs. 3C and 4). Given sufficient discharge and gentle enough slopes for a given b^*, basal shear stress can erode the blockage and heal the channel. Holding all else constant but considering a channel with twice the discharge, the blockage is spread downstream and overbank flow stops (Figs. 3C and 3D). This occurs because, with a higher discharge, the backwater height decreases relative to the flow depth and a smaller

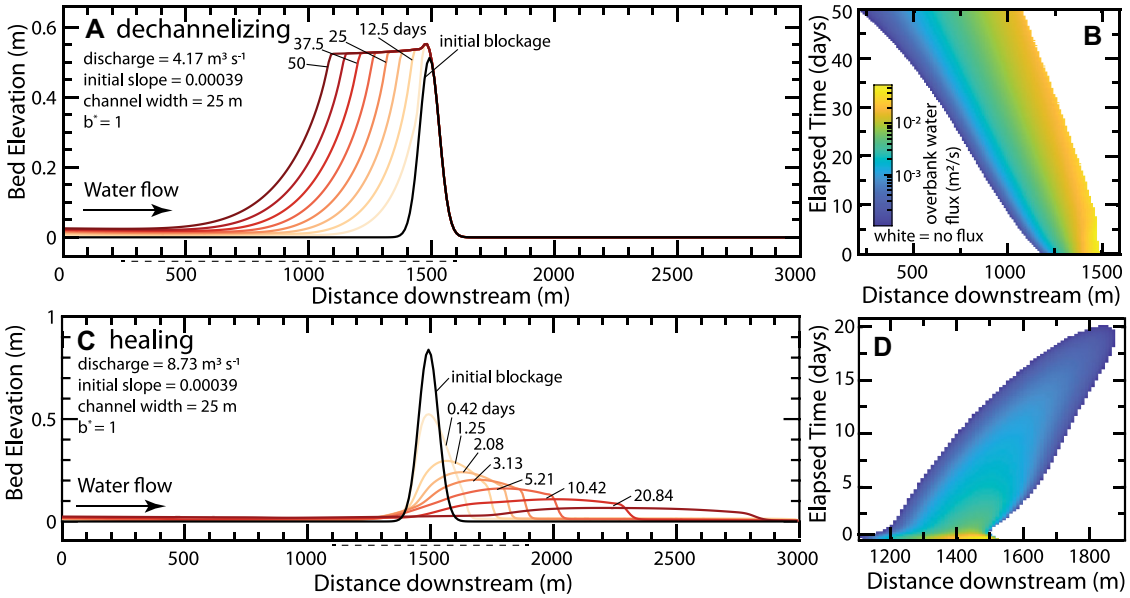

Figure 3. Examples of model output. The initial blockage can lead to (A) upstream-migrating dechannelization or (C) healing as sediment spreads downstream. (B,D) Magnitude and location of overbank flow during the simulations in A and C. Plot extent is marked on the x-axis by a dotted line in A and C. Flux-per-unit levee length is the total going over both levees. Figure 4 shows locations in parameter space.

proportion of the incoming discharge is lost overbank. Increasing b^* moves the threshold for dechannelization to the lower right in Figure 4 because a higher blockage increases overbank flow. Channel width has a minimal effect on the threshold discharge-slope line across the widths tested (see the Supplemental Material).

The field data are generally consistent with the model predictions (Fig. 4). We do not know the blockage height for the field rivers, but assuming $b^* \approx 1$, then 91% (40 of 44 rivers with retrogradational avulsions) plot on the line or within the dechannelizing part of parameter space. Fifty-nine percent (59%) of the field data (26 of 44) plot above $b^* = 0.5$, where the model

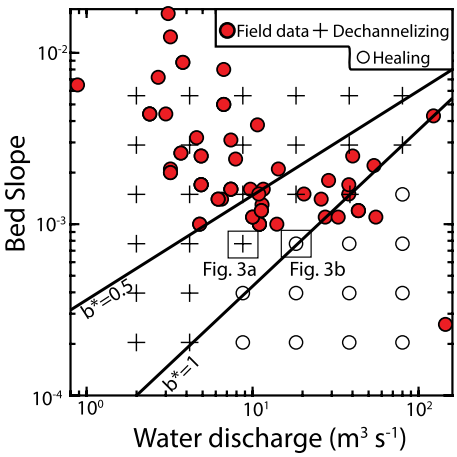

Figure 4. Modeled parameter space. Dechannelizing and healing model runs behave as in Figures 3A and 3B, respectively. Solid lines, which are thresholds between dechannelizing and healing space, change for different nondimensional blockage heights (b^*). Model results shown are for $b^* = 1$ and 25 m channel width. The field data points consist of the 44 unique rivers in our data set; some experienced multiple avulsions.

always predicts dechannelization for runs in this space. Although we assumed that the blockage is sediment, an immobile blockage, such as jammed wood, produces similar results, except channels do not heal because the jam cannot be dispersed. Instead, discharge loss overbank causes alluviation upstream and downstream of the jam. Not all field observations fall within the space defined by the model runs in Figure 4. Model runs were limited to this domain because of numerical instabilities.

IMPLICATIONS FOR AVULSION AND FLOODPLAIN DYNAMICS

Nearly all models assume that avulsions occur when the river bed aggrades by some proportion of its bankfull channel depth (Jerolmack and Mohrig, 2007; Hajek and Wolinsky, 2012). In the case of retrogradational avulsions, the entire channel bed need not aggrade. Instead, retrogradational avulsions should take place on rivers where blockages are prevalent and where the topography slopes away from the channel, preventing water from re-entering immediately downstream of the blockage. Because most aggrading channels have alluvial ridges with transverse slopes, the recurrence of blockages would set the frequency of retrogradational avulsions.

The dechannelization process during retrogradation impacts floodplain ecology and could create distinctive stratigraphic facies. Large-scale forest die-off (Fig. 1H) would allow pioneer species such as mahogany to regenerate (Gullison et al., 1996), which would affect forest biodiversity and succession. Overbank sediment deposition during dechannelization in Bolivia was up to 2 m thick (Lombardo, 2017). Stratigraphically, a channel similar to those of the study areas that filled during retrogradational avulsion would be narrow and show a coarse-grained fill with dimensions that approximate the instantaneous channel form, have vertically aggraded or perhaps upstream-dipping sediment packages, abundant large woody debris, and evidence for rapid deposition (possibly climbing ripples and graded beds). Shallow-flow sheets of sediment would slope gently away from the channel fill, and dead tree trunks would be buried upright. The rapid channel filling during a retrogradational avulsion could generate the suites of small, coarse-grained channel bodies that are often present in alluvial successions. If retrogradational avulsions are caused by logjams, then we would expect this stratigraphic signature to emerge after the evolution of trees in the Middle to Late Devonian.

CONCLUSIONS

We present evidence and a model for a new style of avulsion. Retrogradational avulsions occur when a channel blockage triggers an upstream-migrating wave of dechannelization that forces water overbank and fills the preexisting channel with sediment. The overbank flooding creates a characteristic chevron of dead vegetation and trees adjacent to the channel that is observable in Landsat data. The avulsion completes when overbank flow establishes a new pathway, which is usually through incision into preexisting floodplain or annexation. Retrogradational avulsions tend to form on rivers with small discharges and steep slopes. Model results show that under these conditions a channel blockage maximizes overbank flow loss relative to channelized discharge. This new style of river avulsion is currently unaccounted for in facies models of fluvial fans and may be an important contributor to floodplain aggradation and the architecture of small rivers prone to blockage by sediment and wood. Field studies are needed to evaluate the sedimentary deposits related to this new avulsion style.

ACKNOWLEDGMENTS

D.A. Edmonds, H.K. Martin, R. Henson, and J.M. Valenza were supported by U.S. National Science Foundation grant EAR-1911321. We thank E. Lazarus, an anonymous reviewer, and M. Kleinhans for constructive comments that improved this manuscript.

REFERENCES CITED

Abbe, T.B., and Montgomery, D.R., 2003, Patterns and processes of wood debris accumulation in the Queets river basin, Washington: Geomorphology, v. 51, p. 81–107, https://doi.org/10.1016/S0169-555X(02)00326-4.

Buehler, H.A., Weissmann, G.S., Scuderi, L.A., and Hartley, A.J., 2011, Spatial and temporal evolution of an avulsion on the Taquari River distributive fluvial system from satellite image analysis: Journal of Sedimentary Research, v. 81, p. 630–640, https://doi.org/10.2110/jsr.2011.040.

Collins, B.D., Montgomery, D.R., Fetherston, K.L., and Abbe, T.B., 2012, The floodplain large-wood cycle hypothesis: A mechanism for the physical and biotic structuring of temperate forested alluvial valleys in the North Pacific coastal ecoregion: Geomorphology, v. 139, p. 460–470, https://doi.org/10.1016/j.geomorph.2011.11.011.

Donselaar, M.E., Cuevas Gozalo, M.C., and Moyano, S., 2013, Avulsion processes at the terminus of low-gradient semi-arid fluvial systems: Lessons from the Río Colorado, Altiplano endorheic basin, Bolivia: Sedimentary Geology, v. 283, p. 1–14, https://doi.org/10.1016/j.sedgeo.2012.10.007.

Edmonds, D.A., Hajek, E.A., Downton, N., and Bryk, A.B., 2016, Avulsion flow-path selection on rivers in foreland basins: Geology, v. 44, p. 695–698, https://doi.org/10.1130/G38082.1.

Geertsema, T.J., Torfs, P.J.J.F., Eekhout, J.P.C., Teuling, A.J., and Hoitink, A.J.F., 2020, Wood-induced backwater effects in lowland streams: River Research and Applications, v. 36, p. 1171–1182, https://doi.org/10.1002/rra.3611.

Gullison, R.E., Panfil, S.N., Strouse, J.J., and Hubbell, S.P., 1996, Ecology and management of mahogany (*Swietenia macrophylla* King) in the Chimanes Forest, Beni, Bolivia: Botanical Journal of the Linnean Society, v. 122, p. 9–34, https://doi.org/10.1111/j.1095-8339.1996.tb02060.x.

Hager, W.H., 1987, Lateral outflow over side weirs: Journal of Hydraulic Engineering, v. 113, p. 491–504, https://doi.org/10.1061/(ASCE)0733-9429(1987)113:4(491).

Hajek, E.A., and Edmonds, D., 2014, Is river avulsion style controlled by floodplain morphodynamics?: Geology, v. 42, p. 199–202, https://doi.org/10.1130/G35045.1.

Hajek, E.A., and Wolinsky, M.A., 2012, Simplified process modeling of river avulsion and alluvial architecture: Connecting models and field data: Sedimentary Geology, v. 257, p. 1–30, https://doi.org/10.1016/j.sedgeo.2011.09.005.

Hamilton, P.B., Strom, K., and Hoyal, D.C.J.D., 2013, Autogenic incision-backfilling cycles and lobe formation during the growth of alluvial fans with supercritical distributaries: Sedimentology, v. 60, p. 1498–1525, https://doi.org/10.1111/sed.12046.

Jerolmack, D.J., and Mohrig, D., 2007, Conditions for branching in depositional rivers: Geology, v. 35, p. 463–466, https://doi.org/10.1130/G23308A.1.

Jones, H.L., and Hajek, E.A., 2007, Characterizing avulsion stratigraphy in ancient alluvial deposits: Sedimentary Geology, v. 202, p. 124–137, https://doi.org/10.1016/j.sedgeo.2007.02.003.

Kleinhans, M., De Haas, T., Lavooi, E., and Makaske, B., 2012, Evaluating competing hypotheses for the origin and dynamics of river anastomosis: Earth Surface Processes and Landforms, v. 37, p. 1337–1351, https://doi.org/10.1002/esp.3282.

Kraus, M.J., 1996, Avulsion deposits in lower Eocene alluvial rocks, Bighorn Basin, Wyoming: Journal of Sedimentary Research, v. 66, p. 354–363, https://doi.org/10.1306/D4268347-2B26-11D7-8648000102C1865D.

Linke, S., et al., 2019, Global hydro-environmental sub-basin and river reach characteristics at high spatial resolution: Scientific Data, v. 6, https://doi.org/10.1038/s41597-019-0300-6.

Lombardo, U., 2016, Alluvial plain dynamics in the southern Amazonian foreland basin: Earth System Dynamics, v. 7, p. 453, https://doi.org/10.5194/esd-7-453-2016.

Lombardo, U., 2017, River logjams cause frequent large-scale forest die-off events in southwestern Amazonia: Earth System Dynamics, v. 8, p. 565–575, https://doi.org/10.5194/esd-8-565-2017.

Mackey, S.D., and Bridge, J.S., 1995, Three-dimensional model of alluvial stratigraphy: Theory and application: Journal of Sedimentary Research, B65, p. 7–31, https://doi.org/10.1306/D42681D5-2B26-11D7-8648000102C1865D.

McCarthy, T.S., Ellery, W.N., and Stanistreet, I.G., 1992, Avulsion mechanisms on the Okavango Fan, Botswana: The control of a fluvial system by vegetation: Sedimentology, v. 39, p. 779–795, https://doi.org/10.1111/j.1365-3091.1992.tb02153.x.

Medeiros, S.C., and Hagen, S.C., 2013, Review of wetting and drying algorithms for numerical tidal flow models: International Journal for Numerical Methods in Fluids, v. 71, p. 473–487, https://doi.org/10.1002/fld.3668.

Mohrig, D., Heller, P.L., Paola, C., and Lyons, W.J., 2000, Interpreting avulsion process from ancient alluvial sequences: Guadalope-Matarranya system (northern Spain) and Wasatch Formation (western Colorado): Geological Society of America Bulletin, v. 112, p. 1787–1803, https://doi.org/10.1130/0016-7606(2000)112<1787:IAPFAA>2.0.CO;2.

Phillips, J.D., 2012, Log-jams and avulsions in the San Antonio River Delta, Texas: Earth Surface Processes and Landforms, v. 37, p. 936–950, https://doi.org/10.1002/esp.3209.

Ranga Raju, K.G., Gupta, S.K., and Prasad, B., 1979, Side weir in rectangular channel: Journal of the Hydraulics Division, v. 105, p. 547–554, https://doi.org/10.1061/JYCEAJ.0005207.

Reitz, M.D., and Jerolmack, D.J., 2012, Experimental alluvial fan evolution: Channel dynamics, slope controls, and shoreline growth: Journal of Geophysical Research: Earth Surface, v. 117, F02021, https://doi.org/10.1029/2011JF002261.

Ruiz-Villanueva, V., Piégay, H., Gurnell, A.M., Marston, R.A., and Stoffel, M., 2016, Recent advances quantifying the large wood dynamics in river basins: New methods and remaining challenges: Reviews of Geophysics, v. 54, p. 611–652, https://doi.org/10.1002/2015RG000514.

Smith, N.D., Cross, T.A., Dufficy, J.P., and Clough, S.R., 1989, Anatomy of an avulsion: Sedimentology, v. 36, p. 1–23, https://doi.org/10.1111/j.1365-3091.1989.tb00817.x.

Stouthamer, E., and Berendsen, H.J.A., 2000, Factors controlling the Holocene avulsion history of the Rhine-Meuse delta (The Netherlands): Journal of Sedimentary Research, v. 70, p. 1051–1064, https://doi.org/10.1306/033000701051.

Tooth, S., 2000, Downstream changes in dryland river channels: The Northern Plains of arid central Australia: Geomorphology, v. 34, p. 33–54, https://doi.org/10.1016/S0169-555X(99)00130-0.

Valenza, J.M., Edmonds, D.A., Hwang, T., and Roy, S., 2020, Downstream changes in river avulsion style are related to channel morphology: Nature Communications, v. 11, https://doi.org/10.1038/s41467-020-15859-9.

Van Dijk, M., Kleinhans, M.G., Postma, G., and Kraal, E., 2012, Contrasting morphodynamics in alluvial fans and fan deltas: Effect of the downstream boundary: Sedimentology, v. 59, p. 2125–2145, https://doi.org/10.1111/j.1365-3091.2012.01337.x.

Weissmann, G., Hartley, A., Scuderi, L., Nichols, G., Owen, A., Wright, S., Felicia, A., Holland, F., and Anaya, F., 2015, Fluvial geomorphic elements in modern sedimentary basins and their potential preservation in the rock record: A review: Geomorphology, v. 250, p. 187–219, https://doi.org/10.1016/j.geomorph.2015.09.005.

Wohl, E., 2011, Threshold-induced complex behavior of wood in mountain streams: Geology, v. 39, p. 587–590, https://doi.org/10.1130/G32105.1.

Wohl, E., 2020, Wood process domains and wood loads on floodplains: Earth Surface Processes and Landforms, v. 45, p. 144–156, https://doi.org/10.1002/esp.4771.

Printed in USA